galaxies

MDPI

Review

Opacities and Atomic Diffusion

Georges Alecian [1,†] and Morgan Deal [2,†,*]

[1] Laboratoire Univers et Théories (LUTH), Observatoire de Paris, Université PSL, Université Paris-Cité, Centre national de la recherche scientifique (CNRS), 5 Place Jules Janssen, 92190 Meudon, France; georges.alecian@obspm.fr
[2] Laboratoire Univers et Particules de Montpellier (LUPM), Université de Montpellier, Centre national de la recherche scientifique (CNRS), Place Eugène Bataillon, 34095 Montpellier, France
* Correspondence: morgan.deal@umontpellier.fr
† These authors contributed equally to this work.

Abstract: Opacity is a fundamental quantity for stellar modeling, and it plays an essential role throughout the life of stars. After gravity drives the collapse of interstellar matter into a protostar, the opacity determines how this matter is structured around the stellar core. The opacity explains how the radiation field interacts with the matter and how a major part of the energy flows through the star. It results from all the microscopic interactions of photons with atoms. Part of the momentum exchange between photons and atoms gives rise to radiative accelerations (specific to each type of atom), which are strongly involved in a second-order process: atomic diffusion. Although this process is a slow one, it can have a significant impact on stellar structure and chemical composition measurements. In this review, we discuss the way opacities are presently computed and used in numerical codes. Atomic diffusion is described, and the current status of the consideration of this process is presented.

Keywords: opacities; atomic diffusion; surface abundances; stellar interior; stellar atmosphere

Citation: Alecian, G.; Deal, M. Opacities and Atomic Diffusion. *Galaxies* **2023**, *11*, 62. https://doi.org/10.3390/galaxies11030062

Academic Editor: Dominic Bowman

Received: 31 March 2023
Revised: 18 April 2023
Accepted: 23 April 2023
Published: 25 April 2023

1. Introduction

Knowing how chemical elements are distributed in stellar interiors and atmospheres is crucial in stellar evolution. Hydrogen and helium are the most abundant elements, and heavy elements (or metals) only account for a small percentage of the total mass of stars during the majority of the star's life. However, metals have a strong impact on the stellar structure. Opacity, which quantifies the interaction of photons with matter, results from many atomic processes and affects the transfer of radiation through the stellar layers. Therefore, it is a key ingredient to describe the transport of energy in stars. It depends on the detailed atomic structure of atoms, on the chemical composition, and more specifically, on the mixture of heavy elements. Opacities are thus essential to understanding stellar properties.

The chemical composition inside the star is affected by nuclear processes in the core and by the transport processes of chemical elements outside the core. Macroscopic transport processes act similarly for all elements, while atomic diffusion is selective and affects their distribution. Atomic diffusion, which is mainly driven by the competition between gravity and radiative accelerations, leads to a redistribution of chemical elements from the interior to the atmosphere with timescales from a few Gyr (deep inside the star) to a few years in outer layers. As diffusion timescales increase with depth, the older the star, the deeper the deepest layers that may be affected by diffusion. The modeling of atomic diffusion requires accurate stellar opacities and/or atomic data. Stellar opacities and atomic diffusion are tightly linked. When effective (with weak enough mixing motions), diffusion may have significant consequences on the structure of the star and on its evolution (it affects the age derived for globular clusters for instance). Its modeling is therefore important for stellar

physics and for all studies requiring an accurate understanding of stellar structure and evolution.

In the following, we describe stellar opacities and their implementation in stellar evolution code in Section 2. In Section 3, we describe atomic diffusion and some of the competing macroscopic processes in stellar interiors and atmospheres. Then, we describe the stratification of abundances from the interior to the atmosphere in Section 4. In Section 5, we detail some examples of coupling between transport processes of chemical elements through opacity variations. In Section 6, we briefly discuss radiatively driven wind. Finally, the discussion and conclusions are in Section 7.

2. Stellar Opacities

2.1. Definitions

The mean free path of a photon l with a frequency ν is defined by

$$l_\nu = \frac{1}{n\sigma_\nu}, \tag{1}$$

where n is the number of atoms per unit volume and σ_ν is the cross-section for the absorption of photons at frequency ν. The computation of the frequency-dependent cross-sections includes the contribution of photoionization (bound-free), photoexcitation (bound-bound), inverse Bremsstrahlung (free-free), and photon scattering. An example of $\kappa_\nu = \sigma_\nu/\mu$ for Ca is shown in Figure 1, where μ is the mean molecular weight. An average opacity cross-section σ_R, also called Rosseland mean opacity cross-section, is the harmonic mean of the monochromatic opacity cross-section, weighed by the derivative of the Planck function according to the temperature $\frac{\mathrm{d}B_\nu}{\mathrm{d}T}$,

$$\frac{1}{\sigma_R} = \frac{\int_0^{+\infty} \frac{\frac{\mathrm{d}B_\nu}{\mathrm{d}T}}{\sigma_\nu} d\nu}{\int_0^{+\infty} \frac{\mathrm{d}B_\nu}{\mathrm{d}T} d\nu} = \int_0^{+\infty} \frac{F_u}{\sigma_u} du \tag{2}$$

where $u = \frac{h\nu}{k_B T}$ is the dimension less energy, σ_u is the cross-section for absorption of photons at the dimensionless energy u, with h the Planck constant and k_B the Boltzmann constant, and F_u is the normalized temperature derivative of the Planck function in terms of u see [1].

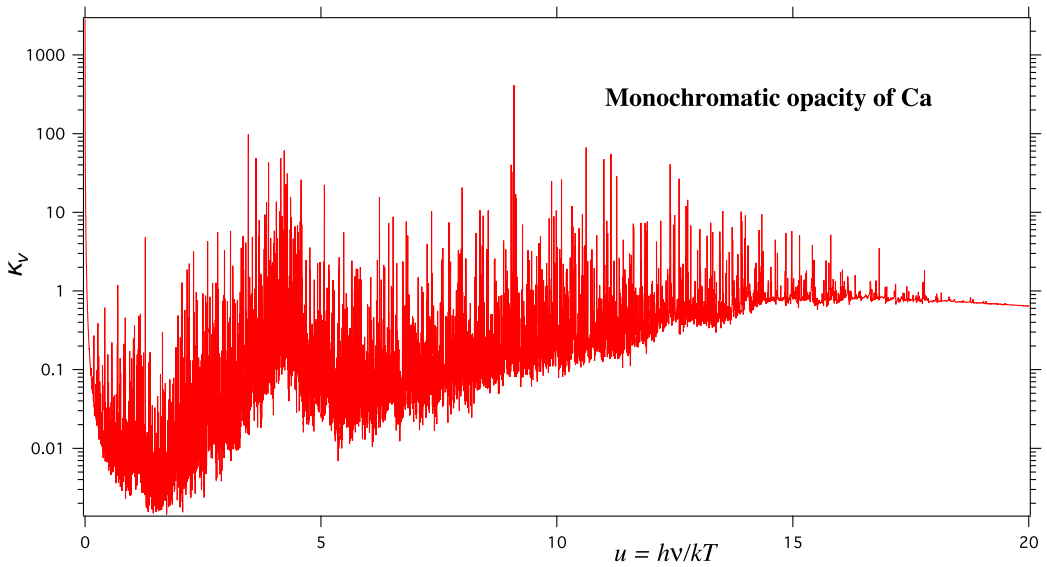

Figure 1. An example of monochromatic opacity. The case of calcium from OP data for a temperature of 10^5 K and density of 7.8×10^{-7} g·cm^{-3}.

The Rosseland mean opacity (cm^2/g) is then written

$$\kappa_R = \sigma_R \frac{n}{\rho} = \frac{\sigma_R}{\mu}, \quad (3)$$

where ρ is the density. The Rosseland mean opacity then depends on the temperature, the density, and the detailed chemical composition. The computation of the cross-sections is very demanding in computation time and requires detailed modeling of the interactions between the radiation and the atoms. This is the reason why such computations cannot be performed on-the-fly in stellar evolution codes.

2.2. Implementation in Stellar Evolution Codes

Stellar evolution equations include the contribution of opacity in the energy conservation equation. Opacities are also needed for the computation of atomic diffusion (see Section 7) and other processes. Because the on-the-fly computation of opacity cross-sections is not possible in stellar evolution codes, the Rosseland mean opacities (or opacity cross-sections) are provided with tables.

The Rosseland mean opacity tables are given as a function of $\log T$ for different values of $\log R$ (with $R = \rho/T_6^3$ and $T_6 = 10^{-6}$ T K). Each of these tables is provided for one combination of (X, Y, Z) with $X + Y + Z = 1$ and Y being the helium mass fraction. In order to cover the wide variety of stars and the variations in stellar interiors, the temperature range generally goes from about $10^{3.5}$ to $10^{8.0}$ K, and the R range from $10^{-8.0}$ to $10^{+1.0}$ 10^{18} $g{\cdot}cm^{-3}{\cdot}K^{-3}$. At low temperatures (<$10^4$ K), the contribution of molecules is important and specific tables need to be included. A list of the available Rosseland mean opacity tables is presented in Table 1.

Table 1. List of available Rosseland mean opacity and opacity cross-section type 1 tables for stellar evolution codes in the literature.

Type of Table	Group	Status	Ref.
Rosseland mean	OP	Public [1]	[2]
-	OPAL	Public [2]	[3]
-	OPAS	Public [3]	[4,5]
-	OPLIB	Public [4]	[6]
-	SCO-RCG	In progress	[7]
low T	Whichita	Public [5]	[8]
-	ÆSOPUS	Public [6]	[9]
Monochromatic cross-sections	OP	Public [1]	[2]
-	OPAL	Not public	[3,10]
-	SCO-RCG	In progress	[7,11]

[1] http://cdsweb.u-strasbg.fr/OP.htx (accessed on 20 April 2023). [2] https://opalopacity.llnl.gov/existing.html (accessed on 20 April 2023). [3] https://cdsarc.cds.unistra.fr/viz-bin/cat/J/ApJS/220/2 (accessed on 20 April 2023). [4] https://aphysics2.lanl.gov/apps/ (accessed on 20 April 2023). [5] https://www.wichita.edu/academics/fairmount_college_of_liberal_arts_and_sciences/physics/Research/opacity.php (accessed on 20 April 2023). [6] http://stev.oapd.inaf.it/cgi-bin/aesopus_2.0 (accessed on 20 April 2023).

All these tables need to be computed with a fixed mixture of metals, most of the time following the solar composition. This gives rise to two main issues: firstly, the open question of the solar abundances proposes to include in the stellar evolution code one set of tables per chemical composition (including the low-temperature tables). Secondly, stellar models computed with these tables should keep the same mixture of metal over the evolution, which is often not the case because of nuclear reactions in the core and transport processes of chemical elements (see Section 3 for the impact of atomic diffusion). This is the reason why, for models with a varying metal mixture over time, the Rosseland mean opacity should be computed at each time step and each mesh point in order to keep the consistency of the internal structure. For that, monochromatic opacity cross-section tables

should be used (see the list at the bottom of Table 1). The difference in the opacity profile when such tables are used is shown in Figure 2. The computation time of models including these tables is larger by a factor of about 10 and they should be used when the variation is large; in other cases, the use of simpler Rosseland mean opacity tables do not significantly affect the accuracy of the models, e.g., [12].

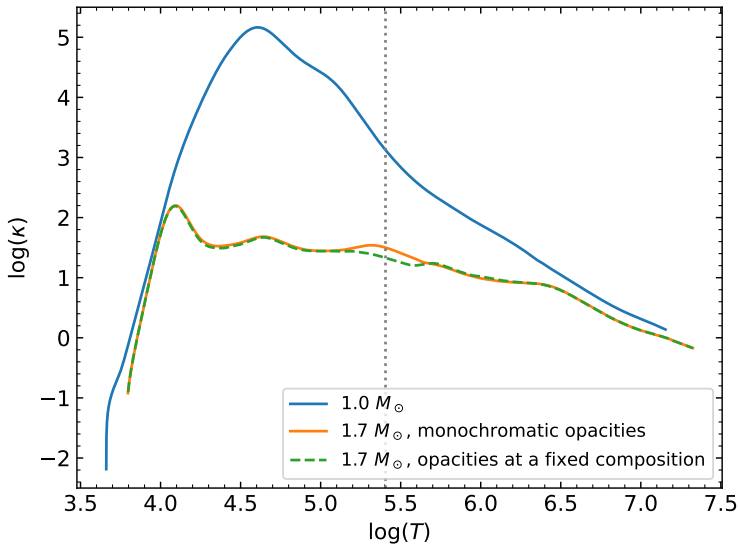

Figure 2. Profiles of the logarithm of the Rosseland mean opacity according to the logarithm of the temperature for 1.0 (blue) and 1.7 $M_\odot$ (orange) models at $X_c = 0.55$. Higher temperatures correspond to deeper layers inside the models. The dashed green curve represents the opacity profile for the same model but using the Rosseland mean opacity not computed from the monochromatic opacities with the exact mixture. The vertical dotted line shows the bottom of the mixed region, where the iron accumulation is induced by radiative acceleration, i.e., where iron is one of the main contributors to the opacity.

2.3. Asteroseismic Constraints on Opacities

The study of the pulsation of stars gives important constraints on their internal structure. The intrinsic oscillation frequencies of stars depend on the properties of the medium they propagate in, hence giving access to information on the inner parts of stars. These pulsations can be driven by different mechanisms depending on the type of pulsator (e.g., β Cephei pulsators and solar-like pulsators).

The Sun is the most studied star, and therefore serves as a reference. Thanks to the high-precision solar data, helioseismology brings strong constraints on the solar internal structure and on solar-like oscillating main-sequence stars in general. Nevertheless, the modeling of the Sun remains a challenge. The inversion of the internal properties of the Sun (thanks to the pressure modes stochastically excited by the convective envelope) shows the need for an increase in theoretical opacities, e.g., [13]. For more massive stars and pulsators such as B-type stars, the pulsations are driven by the κ-mechanism activated by an opacity bump (see, e.g., Section 15.1 of [14] for a description of the mechanism). The understanding of most of the pulsations driven by this mechanism also points toward a current underestimation of the theoretical stellar opacities. The experimental measurement of the iron opacity in the conditions of the base of the solar convective envelope confirmed an underestimation of theoretical opacities between 30 and 400% [15]. The study of stellar pulsations in the Sun and driven by the κ-mechanism is then very important to test the current and future stellar opacity tables.

For example, the origin of some pulsations of the rapidly oscillating Ap[1] stars (roAp), is currently attributed to the κ-mechanism activated by the opacity bump in the hydrogen ionization zone [16,17], with the magnetic field and turbulent pressure also playing an

important role, see [18] for a recent review. For O- and B-type star pulsators, namely β Cephei and SPB[2] stars, the opacity bump is due to iron-peak elements (mainly Fe and Ni), see [19–21]. In the latter example, observations and theoretical predictions suffer from the underestimation of stellar opacities, especially for elements such as Ni and Fe. Ref. [22] showed that an increase of 50–100% of the opacity at the temperature at which the Ni opacity is maximum is needed to understand the pulsations of B-type pulsators of the Magellanic clouds. Ref. [23] showed that for O-type β Cephei stars, an increase of 75% of the iron opacity (which is consistent with the experiment of Bailey et al. [15]) would explain the presence of pulsations in this type of stars.

Revised theoretical opacities are then mandatory for a better understanding of O- and B-type pulsating stars. The OPLIB tables [6] have been tested to model these stars [24]. OPLIB tables predict a larger Rosseland mean opacity than OPAL and OP, leading to wider instability regions. However, all questions cannot be solved by these opacities. Hui-Bon-Hoa et al. [11] compared stellar structure models computed with Ni opacities computed with SCO-RCG [7] and OP. They found that the new Rosseland opacity of Ni is up to a factor of 6 larger than the OP one for $\log(T) < 6$, and the maximum of Ni opacity is also slightly shifted toward lower temperatures. However, the total Rosseland mean opacity is almost not affected by these changes (see Figure 3). Even if these results show that the opacity enhancement is not yet sufficient to explain the pulsation of B-type stars, this opens new possibilities to understand their pulsations and emphasizes the room for improvement in opacity tables.

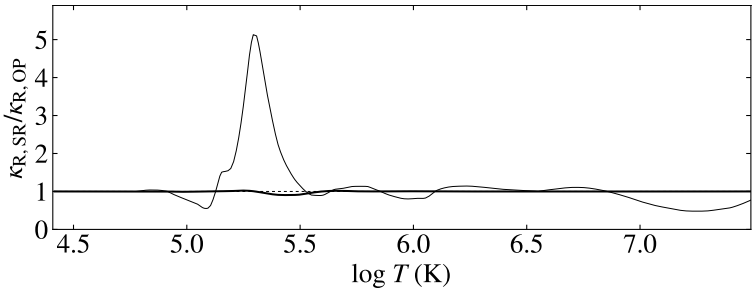

Figure 3. Ratio of the SCO-RCG ($\kappa_{R,SR}$) and OP ($\kappa_{R,OP}$) Rosseland means vs. log T for the stellar mixture (thick line) and for Ni alone (thin line) for a 9.5 $M_\odot$ main-sequence model without atomic diffusion. The dotted line represents a ratio of one. Courtesy of Alain Hui-Bon-Hoa, adapted from [11].

The local enhancement of opacities needed to explain B-type star pulsations may also be partly due to the transport of chemical elements, and especially the effect of atomic diffusion [11,25]. In 2003, Turcotte and Richard [26] showed that chemically peculiar stars of type HgMn overlap the cool side of the HR diagram region of SPB stars. Their numerical simulations showed that HgMn stars should develop Fe accumulation due to atomic diffusion in the iron-bump layers like SPBs. Therefore, these authors proposed that some HgMn stars could pulsate like SPBs. Indeed, photometric variations have been detected in at least two HgMn stars by the CoRoT satellite. However, it has not been established whether these variations are pulsations or rotational modulations [27,28]. Concerning the β Cephei stars, it has been shown by Bourge et al. [29] that atomic diffusion could be responsible for an iron overabundance above the opacity iron-bump zone and thus could affect the spectrum of low radial order eigenfrequencies. Note that atomic diffusion can produce iron overabundances, especially in low metallicity stars such as those of the SMC for which the instability strip should be absent if the iron abundance is homogeneous and identical to the superficial one (see [30]). The fact that some pulsating β Cephei have been observed in the SMC [29] could be explained if, around the iron bump region, layers are stable enough to allow iron accumulation by atomic diffusion.

More recently, it has been shown that the accumulation of Fe and Ni induced by radiative accelerations around $\log(T) \approx 5.2$ combined with thermohaline convection,

e.g., [31–33], a hydrodynamical instability occurring in the presence of an unstable mean molecular weight gradient, led to a local increase in the opacity for A- and B-type stars. Even if the increase occurs at the right temperature inside the star, it is not sufficient to explain the pulsations of B-type stars [34]. Hui-Bon-Hoa et al. [11] emphasize the fact that the radiative acceleration computation of elements such as Ni needs to be refined to draw stronger conclusions. Nevertheless, the transport of chemical elements is an important factor to take into account to solve the long-standing questions about B-type star pulsations.

3. Atomic Diffusion

A stellar plasma is a multicomponent gas in an anisotropic environment where, for instance, temperature and pressure gradients inside a gravitational field contribute to determining the structure of the star. Each of the gas components (particles of the various chemical species, protons, electrons) interacts and exchanges momentum with the others and with photons in a specific way according to its properties, and so, undergoes average forces that differ from those for other components. Therefore, in the absence of matter-mixing motions, there is no reason for the plasma to remain homogeneous. The physical processes describing how the spatial inhomogeneities of the various components may develop in a stellar plasma is called *atomic diffusion*. It is a transport process first considered in the astrophysical context by S. Chapman [35] who first examined the role of thermal diffusion. The theory of atomic diffusion, which is based on the solution of Maxwell–Boltzmann equations (we are in the framework of the kinetic theory of gases), was sometime later detailed in the books of S. Chapman and T.G. Cowling [36], first printed in 1939 and J.M. Burgers [37], with a different approach. Actually, atomic diffusion in stars was neglected in stellar modeling during the first half of the XXth century because it was thought that mixing motions are too strong to allow element separation, see [38,39]. However, gravitational settling (due to atomic diffusion) was considered in 1945 for white dwarfs by E. Schatzman [40].

Atomic diffusion in stellar modeling started to be considered again for main-sequence stars from the pioneering work of G. Michaud [41] in 1970 who gave, for the first time, a convincing solution to the enigma of Ap stars invoking the atomic diffusion process strongly enhanced by radiative accelerations in their atmospheres. Amazingly, radiative acceleration had not been considered by previous works, while it will appear to be the most important ingredient. Because ApBp stars and HgMn stars[3] are slow rotators, and ApBp also have strong magnetic fields, their atmospheres have been shown to be stable enough to allow efficient atomic diffusion processes.

After the work of G. Michaud and mainly during the following decade, many papers dedicated to atomic diffusion in atmospheres of ApBp stars were published, but also for the interiors of Am stars[4]. From the 1990s, much more effort has been put into stellar interiors than atmospheres, not only to study Am stars but also because it was clear that atomic diffusion can affect many other types of stars, the Sun, for instance [42]. Indeed, atomic diffusion may modify the spatial distribution of elements (abundance stratifications) as soon as one has stable radiative layers. Of course, inhomogeneous element distributions inside normal stars are not as impressive as in CP stars; however, some tens of percentages of enhancement/depletion may be found, which may be non-negligible if one considers precise positions of convection zones, evolutionary tracks [10], or precise values of oscillation frequencies for instance. Notice that the time scale needed for elements to stratify varies from some years in the upper atmosphere to more than millions of years in the interior (see Section 4). For a complete discussion of atomic diffusion, the reader can refer to the monograph of [30].

3.1. Main Ingredients to Be Included in Evaluating This Physical Process

Usually, in hydrodynamics, when one speaks about diffusion in a gas or a fluid, one refers to a process that homogenizes the medium and that appears as a second spatial derivative of concentrations in a continuity equation. For instance, if the medium is com-

posed of various types of particles, the concentration of n_k particles of type k is smoothed according to the time by a term $D_k \cdot \partial_z^2 n_k$, where D_k is the diffusion coefficient and z is the spatial coordinate. There is no advection invoked in this process, however, in studies of atomic diffusion in stars, one often speaks about the diffusion velocity of particles of type k. Such a velocity V_{kt} of species k with respect to t type particles was defined by Chapman and Cowling [36] as previously mentioned, see also [43], and may be expressed through:

$$\sum_t \frac{p_k p_t}{p D_{kt}} V_{kt} = A_k \tag{4}$$

where A_k is a term gathering all the forces acting on particles k, D_{kt} the diffusion coefficient of k type particles colliding with a dominant t type particles (generally protons), p_k, p_t, and p are the partial and total pressures, respectively. Here, again, there is no global matter motion in this process, the velocity V_{kt} must be understood as the average velocity of k type particles in the center of mass frame. As soon as the medium is no more isotropic, this average velocity is different from zero. Following the approach of [36,41,44], an algebraic approximation (assuming a plane-parallel medium) of the diffusion velocity of k type particles with respect to protons (p) in stellar interiors may be written as:

$$V_{kp} \approx D_{kp} \left[-\frac{\partial \ln C_k}{\partial r} + \frac{A_k m_p}{kT} \left(g_k^{rad} - g \right) + \frac{(Z_k+1) m_p g}{2kT} + k_T \frac{\partial \ln T}{\partial r} \right], \tag{5}$$

where C_k is the concentration of species k with atomic weight A_k, charge $Z_k e$ (ionization degree times the proton charge), m_p the mass of proton, g_k^{rad} the radiative acceleration, g the gravity, and k_T is a factor for thermal diffusion. Other symbols have their own usual meaning. The first term in brackets will give the smoothing term we mentioned at the beginning of this subsection, the second term represents the competition of radiative acceleration against gravity, the third term is the effect of the electric field[5], the last term is the thermal diffusion.

Actually, in stellar plasma, elements are partially ionized, except very deep inside the star where they become completely ionized (radiative acceleration is then negligible), and where diffusion time-scale becomes very large (larger than the star's lifetime). Generally, if an element k is mainly in an ionization state i at some depth, states $i-1$ and $i+1$ are also present and contribute to the V_{kp}, especially through the radiative acceleration. However, it is not allowed to write a continuity equation using Equation (5) for each ion separately since the population of ions is constrained by the Saha equations. A way to overcome this difficulty is to consider a single velocity equation for element k, assigning an average ionization degree at each depth to it, an average diffusion coefficient, and an average radiative acceleration. This method is discussed and detailed in the book of Michaud et al. [30] (in Section 2.3.3).

The rather simple algebraic expression of the diffusion velocity given by Equation (5) is for stellar interiors, assuming that diffusing element k is a trace element in a plan-parallel medium composed of totally ionized hydrogen. However, to consider more general cases, for instance, in modeling the diffusion of many metals together with He (for which trace element approximation cannot apply), to account for large accumulations of metals at some depth, it is more appropriate to use the Burgers' expressions [37]. This implies solving a system of equations (one by component) to consistently obtain the diffusion velocity of each component simultaneously. This is, of course, a much heavier calculation than using Equation (5), but is necessary for modeling stellar evolution.

For atmospheres, some of the approximations that greatly help calculations in stellar interiors are no more valid, and the Burgers' expressions [37] cannot be used. The fact that a large part of the medium is optically thin and that low ionization degrees have to be considered drastically complicates the calculations, see for instance [45]. Moreover, diffusion velocities become very sensitive to the presence of magnetic fields in atmospheres, the diffusion velocity must be considered as a 2D vector even in plan-parallel modeling

according to the magnetic line inclination. In what follows, we will not discuss atomic diffusion in atmospheres too deeply, but we will mention the notable differences each time it is pertinent.

3.2. Radiative Acceleration

The radiative acceleration of atoms results from their interactions with the radiation field. These interactions are essentially the absorption of photons through bound–bound and bound–free atomic transitions, free–free interactions are generally negligible. The evaluation of radiative acceleration is generally the heavier task in computing diffusion velocities. In this section, we would like to give a short overview of how radiative accelerations may be evaluated, without going too deeply into the numerous technical aspects. A detailed presentation of radiative accelerations may be found in [30].

In an infinite isotropic medium (including the gas of photons), this acceleration is zero. In stars, the radiation flux is not isotropic, and so, radiative acceleration is a non-zero vector oriented as the net radiation flux. A generic algebraic expression for a unique atomic transition may be written as:

$$g^{\mathrm{rad}} = \frac{1}{A m_p c} \int_0^\infty \sigma_\nu F_\nu d\nu \tag{6}$$

where $F_\nu d\nu$ is the net outward radiative energy flux in the frequency range $d\nu$, σ_ν is the absorption cross-section, and c is the velocity of light. Strictly speaking, to have the full radiative acceleration g_k^{rad} of an atom k, one should have to sum over the infinite number of atomic transitions for each ion of k. Of course, in concrete applications, one selects the most contributing bound–bound and bound–free transitions before computing the integrals. Notice an important property of g_k^{rad}: the net radiation flux $F_\nu d\nu$ depends on the concentration of element k since there are less photons available at frequency ν for absorption by each atom k if there are more atoms k. In other words, atoms k must share the available momentum at frequency ν between them. Therefore, g_k^{rad} (average acceleration of each atom k) decreases when C_k increases.

For stellar interiors, there is an equivalent form of Equation (6) in expressing the radiative acceleration of element k that is much more convenient for stellar modeling:

$$g_k^{\mathrm{rad}} = \frac{15}{16\pi^5 r^2} \frac{L_r^{\mathrm{rad}}}{c} \frac{\kappa_{\mathrm{R}}}{X_k} \int_0^\infty \frac{\kappa_{u,k}}{\kappa_{u,\mathrm{all}}} P(u) du \tag{7}$$

with

$$P(u) = u^4 \frac{e^u}{(e^u - 1)^2} \qquad \text{and} \qquad u = \frac{h\nu}{kT} \tag{8}$$

where L_r is the luminosity of the star, X_k is the mass fraction of element k, κ_{R} the Rosseland opacity, $\kappa_{u,k}$ the monochromatic opacity of the element, $\kappa_{u,\mathrm{all}}$ the total monochromatic opacity, all these quantities being estimated at radius r. With this expression, one could take benefit from several numerical opacity databases (for instance, OP, OPAL), where the sum of all contributing atomic transitions is already performed, provided that monochromatic opacity for each element separately is available.

For atmospheres, Equation (7) cannot be used because this expression is only valid in an optically thick medium. Moreover, in atmospheres, there is a complex process of momentum redistribution between the ions of a given element that cannot be accounted for with Equation (7). Generally, methods in evaluating radiative accelerations in atmospheres are much heavier [45,46].

There are several methods for the computation of radiative accelerations, they are detailed and discussed in [30] that we may summarize as follows:

— *Atomic transition approach*. This method consists of calculating explicitly the integral of Equation (6) over the transition probability profile for each atomic transition that is

considered to make a significant contribution to the acceleration. Note that momentum acquired by bound–free transitions of ion i have to be attributed to $i + 1$. This method is most often used for atmospheres [45,46], and no more for interiors after large atomic or opacity data banks became available. With no surprise, this method is the most CPU time-consuming. However, it is, in principle, the most precise one as much as atomic data are accurate and complete.

- *Opacity sampling in stellar evolution*. Here, the radiative acceleration is computed using Equation (7), the method was developed by Richer et al. (1998) [10] and was based on the OPAL database. One of the difficulties of this method is that calculation is performed on a fixed frequency grid, which is most often equally spaced in u, which needs to pay particular attention to the grid resolution. On another hand, this method applies to average atoms (with averaged ionization degree). Notice also that there is a limited number of elements in the databases (mostly elements lighter than Fe), generally elements contributing to the Rosseland average. This implies that studies needing to consider the atomic diffusion of these missing elements cannot be addressed.
- *Interpolation method*. This method was proposed by M. Seaton in 1997 [47]. He was the initiator and the main architect of the Opacity Project (OP). The OP project first consists of computing *ab initio* numerically a large number of atomic transitions for many metals (presently lighter than iron). From these atomic data, the OP team computes tables of opacities (Rosseland average, monochromatic opacities of each element), and the numerical codes allowing interpolation from these tables for any chemical composition and position inside the stars. Since all the necessary data for radiative accelerations are already in the OP database, M. Seaton understood the potential importance of also providing radiative accelerations. He therefore added the codes to compute them with interpolations (as performed for opacities) in a specific table of a function built from Equation (7). This method is accurate and fast compared to the previous ones since all the necessary tables are already computed by the OP team. The method is easy to implement in existing codes. The limit of this method, as previously, is imposed by the list of elements in the database.
- *Semi-analytic or parametric approximation*. The SVP (Single-Valued Parameters) method gives radiative accelerations in stellar interiors without having to explicitly handle large amounts of atomic data or opacity tables. A preliminary version was first proposed by G. Alecian (1985) [48]. In developing Equation (6), one obtains an expression where the atomic data and the concentration of the considered element are mixed, with a non-linear dependence on the concentration. In the SVP approximation, radiative acceleration has an analytic expression where atomic data and concentration are separated. Finally, the part depending on atomic data (which does not change when the concentration changes) may be obtained through pre-calculated small tables with only six parameters per ion [49–51]. This method is the less accurate one; however, it allows very fast computation (10^3 time faster the Seaton's interpolation) and was checked to be accurate enough for modeling stellar evolution [52]. The numerical code and the small table of parameters are provided online [51] presently for 16 elements (more elements should be added in a near future), but when needed for other elements they may be calculated by the user following [49], provided that atomic data are available.

3.3. Atomic Diffusion and Magnetic Fields

There are three main ways by which magnetic fields affect atomic diffusion. The first one has an indirect (but important) influence on the diffusion process. Since stellar matter is essentially composed of charged particles, magnetic fields can impede mixing motions, and hence allow atomic diffusion to build up abundance stratifications.

The second mechanism is microscopic and effective in atmospheres because particle density is small enough there. Indeed, if the collision mean free path of charged particles

is large enough, these particles can spiral enough around magnetic lines to decrease their diffusion coefficient perpendicularly to magnetic lines [36], dividing it by $1 + \omega_i^2 \tau_{\mathrm{col},ip}^2$, where $\tau_{\mathrm{col},ip}$ is the collision time with protons (the time required for collisions to deviate particle i by $\pi/2$), and $\omega_i/2\pi$ the cyclotron frequency. The direct consequence of this effect is to drastically reduce upper atmospheric layers and the vertical diffusion velocity of ions across horizontal magnetic fields.

The third process affecting atomic diffusion is the Zeeman splitting of absorption lines, which may amplify radiative acceleration [46]. According to the Zeeman patterns, the splitting of absorption lines can lead strong lines (which are the main contributors to the radiative acceleration) to desaturate, and therefore, to increase the radiative acceleration. In principle, this effect exists anywhere in the star according to magnetic field intensity; however, its efficiency is significant when line profiles are narrow[6]. Therefore, it essentially concerns diffusion in atmospheres.

3.4. Competition with Macroscopic Motions

We often mention in this section the important role of mixing, since atomic diffusion is a very slow process its effects can only be revealed if mixing is very weak or inexistent. Mixing in stars is a macroscopic hydrodynamical process that may be due to various physical processes; therefore, the subject is extremely broad and cannot be exhaustively addressed here. However, as for many other aspects presented in this section, one can find a relatively detailed discussion in the monograph of Michaud et al. (2015) [30], Chapter 7. Besides mixing, we include in this subsection stellar mass loss, which is also a macroscopic matter flow that competes with atomic diffusion. These competing processes may be summarized as follows (for the majority of them in the present context):

- *Meridional Circulation*. This process is directly linked to star rotation. It is a large-scale motion that transports matter between the pole and the equator and may go deep inside the star. It is stronger as rotation is faster, and according to the efficiency of the kinetic momentum extraction, this could be why chemically peculiar stars are slow rotators. In slow-rotating stars (with types A V or B V), it is believed that meridional circulation is too weak to prevent the gravitational settling of He; Therefore, this diffusion produces the under-abundance of the element. The consequence is that the superficial He convection zone may disappear, and then external layers become stable enough for diffusion.
- *Turbulence*. This is of course the most trivial mixing process since it involves small scales and advective motions. E. Schatzman (1969) [53] proposed to model its effect as a diffusive term. Therefore, he introduced the turbulent diffusion coefficient D_{T} that leads to modify Equation (5) by writing the pure diffusive term as $-\left(D_{kp}+D_T\right)\frac{\partial \ln C_k}{\partial r}$ instead of $-D_{kp}\frac{\partial \ln C_k}{\partial r}$. D_{T} is assumed to be the same for all elements. In the case of perfect mixing, it should be infinite, and zero in a perfectly stable medium. Actually, this coefficient is difficult to estimate. Generally, it is parametrized in the modeling to ensure a soft transition between a mixing and a stable zone, see for instance [54].
- *Convection*. Convection is a very common process in stars and has an important role in models, including atomic diffusion. One may say that it is at the basis of our definition of what we call *normal* stars. In the absence of convection, possibly all slowly rotating stars would have been more or less like chemically peculiar stars, i.e., with a large variety of superficial chemical compositions. If one limits ourselves to the usual convection determined by the Schwarzschild criterion, models including diffusion are strongly constrained by the precise positions of convection zones (CZ). Inside a CZ, the matter is assumed well-mixed (homogeneous abundances); however, its chemical composition is affected by how abundances are stratified by diffusion in the radiative zone just below. This chemical composition is supposed to reflect (with some dilution depending on the mass of the CZ) the composition of the last stable layers before it. Therefore, the parametrization of D_{T} is crucial since it determines the

real position of the bottom of the mixing zone. In ApBp stars, the superficial CZ is assumed non-existent or very small. Therefore, diffusion is extremely efficient directly in the atmosphere, hence producing spectacular abundance anomalies.

– *Mass loss*. This is not a mixing process, but its effect on abundance anomalies may be comparable. In models including atomic diffusion, mass loss is a global outflow of matter. Assuming that it is permanent, stationary, and the star spherical, without magnetic fields, it is modeled as a constant flux of matter (a wind) determined by a unique parameter: the rate of mass loss. At a given radius r with matter density ρ inside a star of mass M_*, it is easy with the assumptions to determine the velocity of the flow to be $(dM_*/dt)/4\pi\rho r^2$. It appears that this velocity may be comparable, at certain depths, to that of diffusion in A- and B-type main sequence stars. If the rate of mass loss is too great (e.g., greater than about 10^{-12} solar mass per year), the mass loss flux brings in new material from deeper parts of the star faster than diffusion can change the local composition, thus preventing abundance stratification. In particular, it is believed that the CP stars phenomenon does not extend to stars hotter than about $T_{\rm eff} \approx 18{,}000$ K because of their strong mass loss. Several studies show that the CP star phenomenon is better reproduced by models if atomic diffusion is combined with mass loss rates around 10^{-13}–10^{-14} solar mass per year see for instance [55,56].

4. Stratification of Abundances across the Star

Atomic diffusion leads to an abundance stratification that depends on the balance between radiative accelerations and gravity. For low mass stars (G-type and cooler), the surface convective zone is deep enough so that, at the base of the convective envelope, radiative accelerations are negligible compared to the local gravity. Moreover, the diffusion timescale is a few Gyr so the abundance variations are small. For a 1.0 $M_\odot$ star, this leads to a slight decrease in the abundance of all elements from the surface (except hydrogen) as seen in the convective envelope of the model shown in Figure 4. As a comparison, the profile variation is much larger in the core for the elements involved in nuclear reactions. Above $r = 0.2$ $R_\odot$, the metal distribution is almost not affected and the surface abundances are close to the initial ones. To do a parallel with the previous part on stellar opacities, the use of opacity tables at fixed mixture is suitable for this type of star.

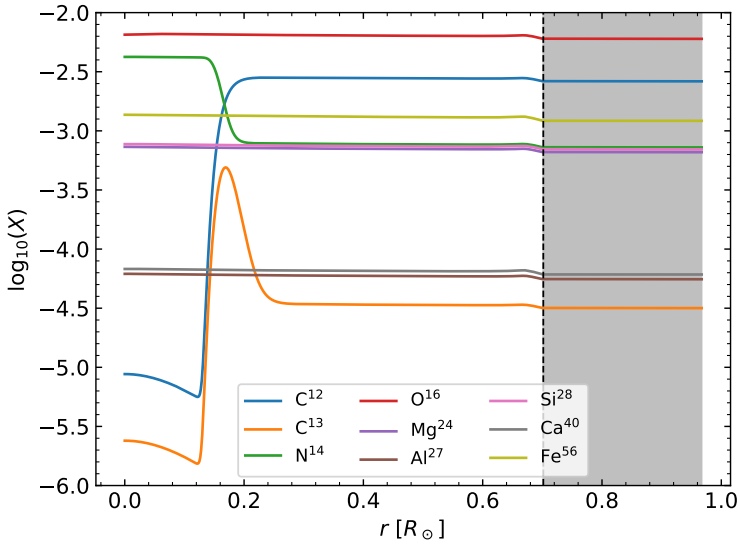

Figure 4. Profiles of the logarithm of the mass fraction according to the radius of several elements for a 1.0 $M_\odot$ model corresponding to ages of 3.48 Gyr. The model is computed with the Cesam2k20 stellar evolution code [52,57,58]. The track is not calibrated on the Sun. The grey area represents the convective region. The vertical dash line represents the boundary between convective and radiative zones.

The picture is different for more massive stars. When the convective envelope becomes shallower (due to the gravitational settling of He because of slow rotation), radiative accelerations start to play an important role in abundance stratification. Some elements accumulate just below the bottom of the superficial convection zone while others are depleted, with much smaller diffusion timescales at this depth. This may significantly modify the superficial chemical composition. Figure 5 shows the abundance profiles for a 1.7 $M_\odot$ model. In addition to atomic diffusion, the model includes turbulent mixing according to the parameters determined for Sirius A [55]. For this model, the most abundant metal at the surface is iron and not oxygen. Aluminum, silicon, and magnesium are also accumulated at the surface. Calcium is depleted at the surface but accumulated below the convective envelope around $r = 1.50$ $R_\odot$ at $X_c = 0.45$ ($r = 2.50$ $R_\odot$ at $X_c = 0.05$). The surface abundance variations are of the same order of magnitude as the variations induced by the nuclear reactions. For a star with a mass of 5.0 $M_\odot$, the results are qualitatively similar, with a more extended convective core, shallower convective envelope, and smaller abundances variations at the surface due to a shorter evolution timescale than for a 1.7 $M_\odot$ star (see Figure 6). In both cases, the use of an opacity table to fix the metal mixture is not suitable for accurate modeling of the stellar interior.

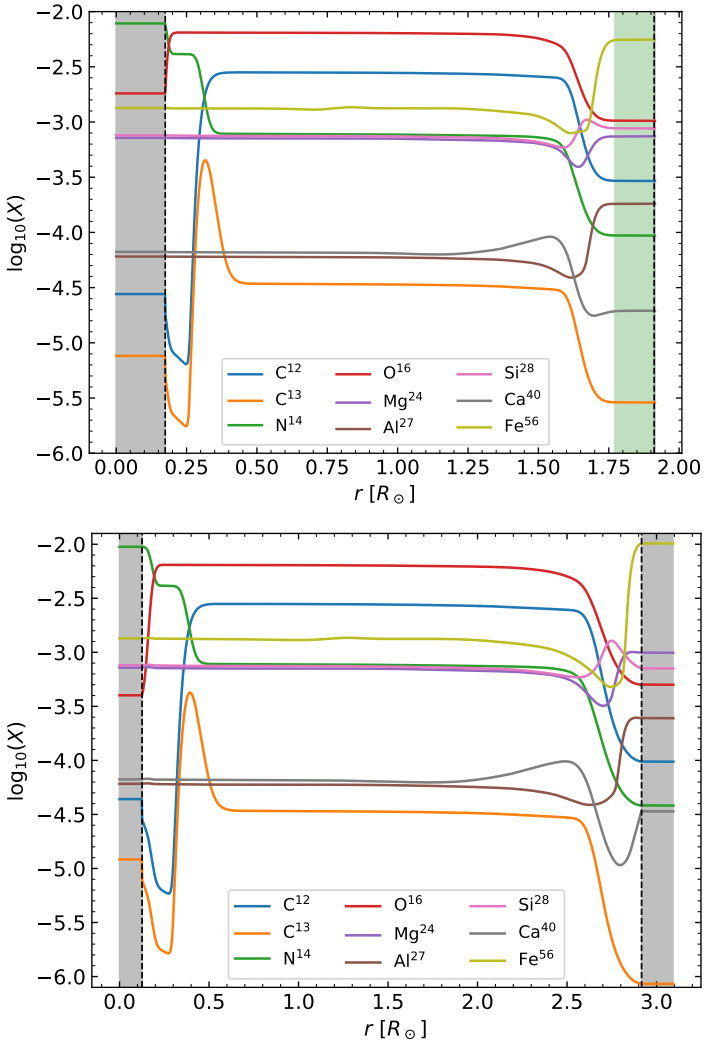

Figure 5. The same legend as Figure 4 for 1.7 $M_\odot$ models at $X_c = 0.45$ (**top panel**) and $X_c = 0.05$ (**bottom panel**). The ages are 0.98 Gyr and 1.76 Gyr, respectively. The grey and green areas represent the convective and turbulent mixing regions, respectively. In the bottom panel, the turbulent mixing region is located inside the convective envelope.

For slowly rotating magnetic stars that are more massive than 1.7 $M_\odot$, it is possible that their atmosphere is stable enough to allow atomic diffusion in building up abundance stratifications in upper layers. 1.7 $M_\odot$ is the lower mass boundary from which the CP stars phenomenon starts to appear: roAp and Ap, followed by the Bp's'. The stability of their atmosphere is confirmed by observations, see for instance [59]. Such a stratification of metals could not be explained if mixing would exist. Before this observational confirmation, the stability of the atmosphere of the Ap star was just the hypothesis needed by theoretical models with atomic diffusion in explaining these stars. Because particle density is much smaller in atmospheres, diffusion velocities are much higher, and diffusion timescales are much shorter. The consequence is that abundance anomalies (overabundances and underabundances) are much stronger. Moreover, since these stars have strong magnetic fields, in addition to vertical stratifications, metals are no more uniformly distribute above the stellar surface. Clouds of metals should be distributed according to the magnetic structures. As written in Section 3.1, we will not detail the atmospheric cases in this chapter; however, to illustrate this domain, we show the case (Figure 7) of a chromium cloud that is due to atomic diffusion in a magnetic atmosphere of $T_{\rm eff} = 12{,}000$ K, and $\log g = 4.0$, assuming an anisotropic wind. This 3D model is a stationary solution obtained from time-dependent calculation of continuity equation (self-consistent model of atmosphere and polarized radiation transfer calculation including Zeeman effect for radiative accelerations) was published by Alecian and Stift (2021) [60].

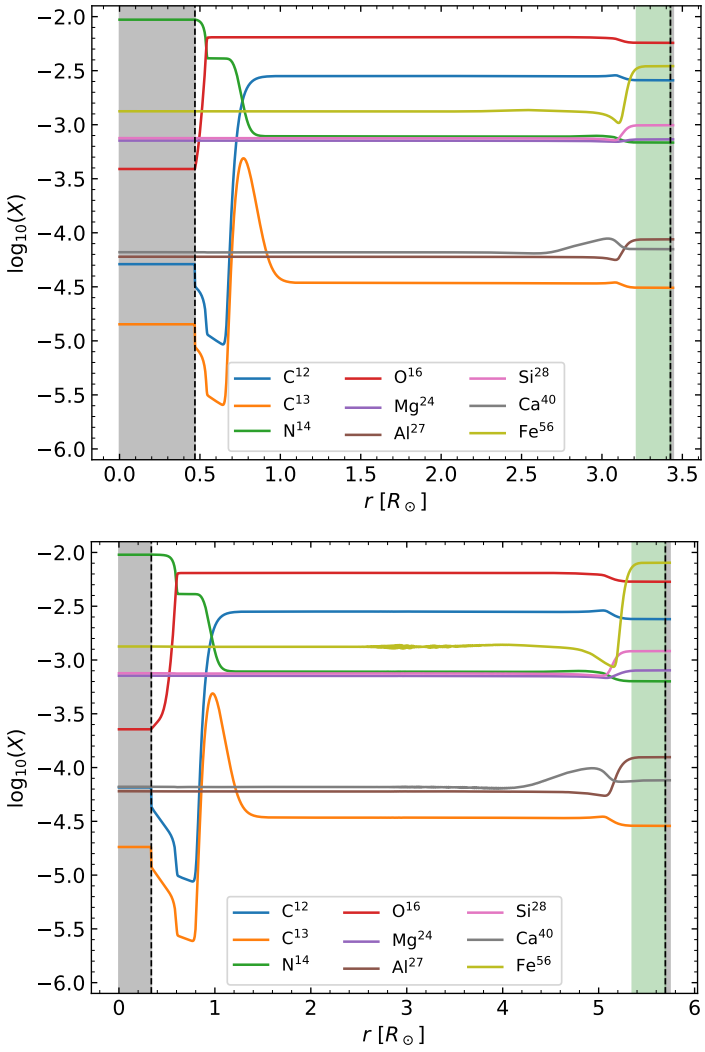

Figure 6. Same legend as Figure 5 for 5.0 $M_\odot$ models. The ages are 57 Myr and 96 Myr, respectively.

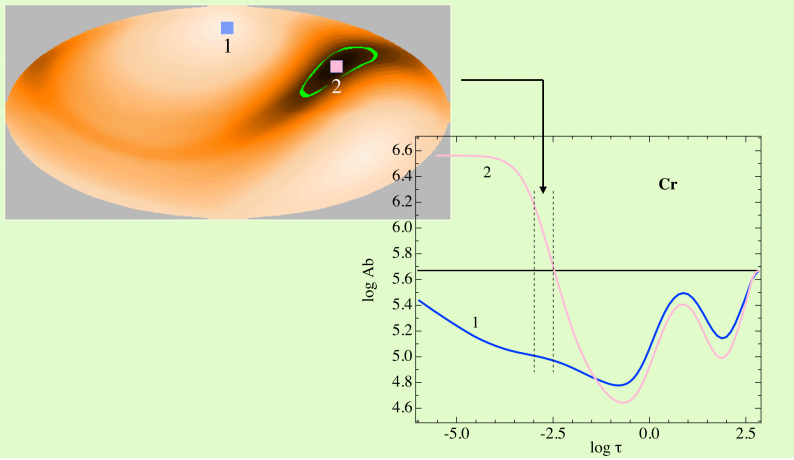

Figure 7. Chromium cloud in an atmosphere $T_{\rm eff} = 12{,}000$ K, and $\log g = 4.0$, assuming an anisotropic wind. The top panel shows the positions (point 1 and point 2) for probing the atmosphere (Hammer projection of the full stellar surface). The right panel presents the chromium abundance stratifications at the last time step, the blue line corresponding to point 1, the pink line to point 2. The horizontal solid black line represents the initial solar abundance. The vertical dashed lines show the depth limits of the slab shown in the top panel.

For non-magnetic slowly rotating stars with the same masses as above, a superficial convection zone may exist. For $T_{\rm eff} < 10{,}000$ K, the bottom of this CZ goes deeper than the atmosphere, but it is not so deep as for normal stars; hence, these stars are also CP stars. They are the AmFm stars with relatively milder abundance anomalies. Above $T_{\rm eff} \approx 10{,}000$ K, we find the HgMn stars, which have stable atmospheres and where atomic diffusion is in play, producing strong abundance anomalies such as ApBp stars, but without magnetic fields.

Horizontal-Branch, and More Evolved Stars

Horizontal-Branch stars (HB) are evolved stars with masses smaller than about two solar masses, which are going to evolve toward the asymptotic giant branch of the HR diagram. At the beginning of the HB phase, these stars are characterized by a He-burning core, below a H envelope. The concentration of carbon in the core increases during the evolution (those of nitrogen and oxygen also but to a lesser extent), and helium gradually disappears in the inner core. Michaud et al. [61] have quantitatively estimated the role of atomic diffusion on the structure of those stars. Because atomic diffusion transports matter through the borders of these different zones, it refuels the nuclear reactions. This affects, for instance, the luminosity and duration of the evolution sequences of the HB stars. Since some methods of determining the distance of globular clusters are based on the HB luminosity, this may indirectly affect the age estimate of the clusters [62,63]. Radiative accelerations or opacities are not involved in what happens at the borders of these different zones, since the concerned layers may be considered fully ionized. This is, however, not the case when one considers the H envelope of HB stars.

Noting that HB stars sequence in the HR diagram crosses the main sequence at regions populated by HgMn and AmFm chemically peculiar stars, Michaud and Richer [64] estimated the effect of atomic diffusion (including radiative accelerations of metals) assuming a similar envelope model as for AmFm stars (comparable $T_{\rm eff}$ and $\log g$), i.e., with the diffusion of metals just below a H convection zone. They obtained metal overabundances in the outer layers of their model, giving so an explanation of those observed by Behr [65]. Of course, the model was simple and could only give trends. On another hand, Khalack et al. [66] found

vertical stratification of iron in the atmosphere of blue HB stars (BHB), which shows that atomic diffusion is efficient in the atmosphere of these stars (they have $T_{\rm eff}$ closer to those of HgMn stars). Theoretical models by Hui-Bon-Hoa et al. [67], LeBlanc et al. [68], Leblanc et al. [69] had given such a trend of metals stratifications in these atmospheres, and have explained the photometric jumps and gaps observed in BHB stars. A detailed review of atomic diffusion in horizontal branch stars can be found in chapter 12 of Michaud et al. [30].

Of the evolved stars where atomic diffusion is clearly effective in stratifying elements, white dwarfs are of particular importance. Indeed they are the first stars for which atomic diffusion has been identified as being able to play an important role in stellar physics. Schatzman [40] in 1945, has shown that the almost pure hydrogen observed in the spectrum of some white dwarfs (DA white dwarfs actually) is the consequence of the gravitational settling of heavier elements (see also Schatzman [70]). In other words, the hydrogen is floating in their atmosphere. A lot of theoretical works have followed this study, and, as knowledge about white dwarfs has progressed, particularly about their status in stellar evolution, it was shown how element stratifications in them depend on effective temperature. Fontaine and Michaud [71] have shown that radiative acceleration in their extremely thin atmosphere is no more negligible for $T_{\rm eff} > 20{,}000$ K, and $T_{\rm eff} > 38{,}000$ K for DB white dwarfs which have a hydrogen convection zone at their surface for cooler $T_{\rm eff}$. Here, again, a detailed review of atomic diffusion in white dwarfs can be found in Michaud et al. [30] (Chapter 13).

5. The Opacity as Vector of Coupling between Transport Processes

The opacity is directly linked to the chemical composition. Any change in the metal mixture affects it and can lead to interesting coupling between transport processes. Such coupling mainly occurs where the metal mixture is strongly affected by atomic diffusion.

The first example is the coupling between atomic diffusion and convection. Radiative accelerations induce local accumulations of chemical elements, where they are the main contributors to opacity. When an accumulation of iron is located in the convective envelope, or close to it, it induces a local increase in the opacity (see Figure 8). This then leads to an increase in the mass of the surface convective zone up to a factor of two depending on the initial chemical composition of the star [52,72]. In more massive stars, the accumulation of iron and nickel induces the so-called iron–nickel convective zone (around $T = 20{,}000$ K) below the hydrogen–helium ones [31,33,73].

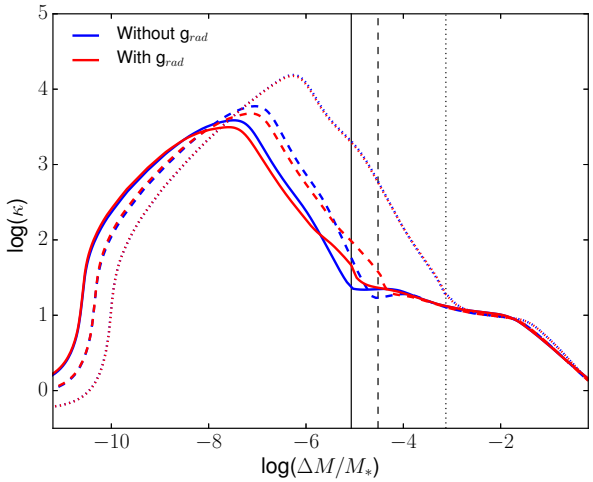

Figure 8. Rosseland mean opacity profiles of 1.4 $M_\odot$ models with $X_c = 0.6$ (solid curves), $X_c = 0.4$ (dashed curves), and $X_c = 0.2$ (dotted curves) from [52]. The blue and red curves represent, respectively, the models without and with radiative accelerations taken into account in the diffusion velocity. The solid dashed and dotted vertical lines represent the positions of the bottom of the surface convection zone for the model without radiative accelerations for the same value of X_c as the opacity profiles (for clarity, they are not represented for the model with grad). Adapted from Figure 5 of [52].

Another example is the coupling between atomic diffusion and rotation. In Section 3.4, we mentioned that rotation attenuates the effect of atomic diffusion, but not suppressing it completely. For F-type stars, atomic diffusion starts to be slightly more efficient than rotation in transporting chemical elements, leading to an accumulation of iron. Again, the local increase in the opacity induces the deepening of the surface convective zone. Rotation-induced mixing strongly depends on the extraction of angular momentum through the magnetized wind at the surface (magnetic braking), and hence the size of the surface convective zone. In this case, magnetic braking is then slightly more efficient thanks to the effect of atomic diffusion and, as a consequence, the rotation-induced mixing is also slightly more efficient [74].

6. Radiatively Driven Winds

The stellar wind observed in O and early B-type stars has been shown to be due to the interaction of the radiation field with metals through their bound–bound atomic transitions. This mechanism was first proposed by Lucy and Solomon [75] who demonstrated (steady-state model) that the scattering of photons in strong lines can be enough to maintain an outflow of matter. Therefore, one speaks of radiatively driven wind. As far as this process is related to the interactions of photons with atomic transitions, it is connected to opacities. However, it is even more connected to atomic diffusion (Section 3) as far as it involves the same important ingredient: radiative acceleration. The study of the mechanism of radiatively driven wind needs to consider detailed radiation transfer in an optically thin expanding atmosphere (in non-local thermodynamic equilibrium condition, hereafter NLTE) where strong velocity gradients cause a desaturation process of strong lines due to the Doppler effect. It also needs to consider how the momentum acquired by heavy metallic ions is efficiently transferred to hydrogen and helium to create a global matter outflow. One could roughly say that the momentum transfer from metals to *passive* atoms (hydrogen and helium) through Coulomb's interactions is much stronger than for atomic diffusion in layers where this process may produce chemical elements stratification. This momentum transfer drags the whole matter of hot stars to outer layers and determines the mass loss rate. Following the work of Lucy and Solomon [75], the theoretical models were improved by Castor et al. [76], Abbott [77], enlightening the role of a large number of weak transition lines. In 1996, Babel [78] showed that for late B-type stars, the metallic components of the wind may decouple from hydrogen for cooler stars (A- and late B-type stars), leading in some cases to the pure metallic wind. The efficiency of momentum transfer from active (ions of metals) to passive components has been studied in more detail by Krtička and Kubát [79], Krtička et al. [80]. To have a quantitative estimate rate of mass loss rate according to the star type is a difficult task: the process is complex and needs considering NLTE effects, and magnetic fields introduce geometric inhomogeneity which leads to going beyond 1D modeling (see for instance Fišák [81]). In addition, observational data are relatively poor in constraining models, especially for late-type stars.

7. Discussion and Conclusions

Stellar opacities are fundamental ingredients of stellar evolution because they control the transport of energy. They depend on the complex interactions between photons and atoms, and on the detailed chemical composition. In numerical modeling, one generally considers only the main contributors to the opacity (about 20 elements). Stellar evolution codes include opacity in the form of tables with a fixed mixture of heavy elements. When the mixture is modified by internal transport processes of chemical elements, the Rosseland mean opacity has to be computed again from monochromatic opacity tables, at each time step and each mesh point. With the current discrepancy between helioseismology and solar models (the so-called *solar problem*), the present opacity tables are questioned through the determination of solar chemical composition.

There is a direct link between stellar opacities and the transport processes of chemical elements, which, in the case of efficient atomic diffusion, modifies the local chemical

composition, and therefore, the Rosseland opacity. Atomic diffusion selectively transports chemical elements, and it is at the origin of most of the chemically peculiar stars. It is in competition with several processes such as convection, large-scale motions induced by rotation, turbulence, magnetic field, and mass loss. One of the main ingredients determining the diffusion velocities is radiative acceleration, which comes from the exchange of momentum between photons and ions. The computation of radiative accelerations requires accurate atomic data and/or stellar opacities tables. Accumulations of metals, induced by radiative accelerations, that contribute the most to the opacity increase the Rosseland mean in the concerned layers. This establishes a dependence between microscopic and macroscopic transport processes that affect the internal structure of stars.

We know from the work of G. Michaud [41] in 1970 that atomic diffusion with radiative accelerations is responsible for the spectacular phenomenon of chemically peculiar stars, especially for those having stable atmospheres. Presently, because of the difficulty in numerical modeling of this process, it is not yet possible to model in detail the atmosphere of a given observed star. This is mainly due to the extreme sensitivity of abundance stratification build-up to macroscopic motions, which are presently difficult to measure in real atmospheres, and therefore, are treated as free parameters. However, numerical models help in understanding the main trends of observed anomalies. Actually, one knows that what happens in the atmosphere does not generally significantly affect the star structure. However, understanding the main trends is important for making various diagnostics since the stellar chemical composition is essentially estimated (from observed spectra) through abundances in atmospheres. Therefore, one needs to be careful when these abundances are considered to be those in deeper layers of the star.

The problem is different for stellar interiors for which macroscopic motions are better constrained in models, and numerical modeling of atomic diffusion is easier since radiative accelerations may be computed from large opacity databases.

The recent asteroseismology surveys such as CoRoT, *Kepler*, TESS, and in the future, PLATO have emphasized the need for accurate stellar evolution models for the accurate determination of stellar systems. Transport processes and stellar opacity play an important role, especially in the determination of accurate stellar age, which can only be obtained from models. It has been shown that neglecting atomic diffusion can lead to errors up to 16%, 2.1%, and 0.8% on the age, the mass, and the radius of solar-like stars, respectively [82]. Neglecting radiative accelerations for stars more massive than the Sun also impacts the stellar ages up to 9% [52]. Atomic diffusion has also been shown to have an influence on the pulsations of more massive stars, such as γ Dor stars, and hence on the determination of their fundamental properties [83]. The contribution of all transport processes of chemical elements is different for each type of star and acts differently on the surface abundances. The effect of atomic diffusion is always present at different levels and should not be neglected in the modeling of stars, especially in the era of high-precision observations that require high-accuracy stellar models. The accurate modeling of atomic diffusion and opacities in stellar evolution models is then essential to achieving the 10% PLATO/ESA requirement on the ages of stellar systems similar to the solar one.

Author Contributions: G.A. and M.D. contributed equally to this work. All authors have read and agreed to the published version of the manuscript.

Funding: This research received no external funding.

Data Availability Statement: Not applicable.

Conflicts of Interest: The authors declare no conflict of interest.

Notes

[1] A group of main-sequence magnetic and chemically peculiar stars (CP stars) of type A.

[2] Slowly Pulsating B-type stars.

[3] Groups of main-sequence CP stars of types A and late B, showing the strongest abundance anomalies in their atmospheres. In these stars, some elements are underabundant, but most heavy metals are overabundant by several orders of magnitude with respect to solar abundances: for instance Fe may be 10^2 time overabundant, Hg up to 10^5 time!

[4] Group of main-sequence CP stars of type A, with milder abundance anomalies than the groups previously mentioned.

[5] Electric field is due to the relative diffusion of protons and electrons due to the gradient of the total pressure, it was introduced by [44].

[6] We are speaking about local line profile (not the observed one), i.e., the absorption profile of the net radiation flux at radius r (even in optically thick depth), and at the absorption frequency. Below atmosphere, due to an increase in the collisional broadening of transition probability profile, saturation of lines decreases, and Zeeman splitting has much less effect on radiative acceleration.

References

1. Badnell, N.R.; Bautista, M.A.; Butler, K.; Delahaye, F.; Mendoza, C.; Palmeri, P.; Zeippen, C.J.; Seaton, M.J. Updated opacities from the Opacity Project. *MNRAS* **2005**, *360*, 458–464.
2. Seaton, M.J. Opacity Project data on CD for mean opacities and radiative accelerations. *MNRAS* **2005**, *362*, L1–L3.
3. Iglesias, C.A.; Rogers, F.J. Updated Opal Opacities. *ApJ* **1996**, *464*, 943. [CrossRef]
4. Blancard, C.; Cossé, P.; Faussurier, G. Solar Mixture Opacity Calculations Using Detailed Configuration and Level Accounting Treatments. *ApJ* **2012**, *745*, 10. [CrossRef]
5. Mondet, G.; Blancard, C.; Cossé, P.; Faussurier, G. Opacity Calculations for Solar Mixtures. *ApJS* **2015**, *220*, 2. [CrossRef]
6. Colgan, J.; Kilcrease, D.P.; Magee, N.H.; Sherrill, M.E.; Abdallah, J.J.; Hakel, P.; Fontes, C.J.; Guzik, J.A.; Mussack, K.A. A New Generation of Los Alamos Opacity Tables. *ApJ* **2016**, *817*, 116.
7. Pain, J.C.; Gilleron, F. Accounting for highly excited states in detailed opacity calculations. *High Energy Density Phys.* **2015**, *15*, 30–42.
8. Ferguson, J.W.; Alexander, D.R.; Allard, F.; Barman, T.; Bodnarik, J.G.; Hauschildt, P.H.; Heffner-Wong, A.; Tamanai, A. Low-Temperature Opacities. *ApJ* **2005**, *623*, 585–596.
9. Marigo, P.; Aringer, B.; Girardi, L.; Bressan, A. Low-Temperature Gas Opacities with AESOPUS 2.0. *arXiv* **2022**, arXiv:2210.08587.
10. Richer, J.; Michaud, G.; Rogers, F.; Iglesias, C.; Turcotte, S.; LeBlanc, F. Radiative Accelerations for Evolutionary Model Calculations. *ApJ* **1998**, *492*, 833–842. [CrossRef]
11. Hui-Bon-Hoa, A.; Pain, J.C.; Richard, O. New nickel opacities and their impact on stellar models. *A&A* **2022**, *658*, A70.
12. Hui-Bon-Hoa, A. Stellar models with self-consistent Rosseland opacities. Consequences for stellar structure and evolution. *A&A* **2021**, *646*, L6. [CrossRef]
13. Buldgen, G.; Salmon, S.J.A.J.; Noels, A.; Scuflaire, R.; Montalban, J.; Baturin, V.A.; Eggenberger, P.; Gryaznov, V.K.; Iosilevskiy, I.L.; Meynet, G.; et al. Combining multiple structural inversions to constrain the solar modelling problem. *A&A* **2019**, *621*, A33.
14. Maeder, A. *Physics, Formation and Evolution of Rotating Stars*, *Astronomy and Astrophysics Library*; Springer International Publishing: Cham, Switzerland, 2009. [CrossRef]
15. Bailey, J.E.; Nagayama, T.; Loisel, G.P.; Rochau, G.A.; Blancard, C.; Colgan, J.; Cosse, P.; Faussurier, G.; Fontes, C.J.; Gilleron, F.; et al. A higher-than-predicted measurement of iron opacity at solar interior temperatures. *Nature* **2015**, *517*, 56–59. [CrossRef] [PubMed]
16. Balmforth, N.J.; Cunha, M.S.; Dolez, N.; Gough, D.O.; Vauclair, S. On the excitation mechanism in roAp stars. *MNRAS* **2001**, *323*, 362–372. [CrossRef]
17. Saio, H. A non-adiabatic analysis for axisymmetric pulsations of magnetic stars. *MNRAS* **2005**, *360*, 1022–1032. [CrossRef]
18. Holdsworth, D.L. The roAp Stars Observed by the Kepler Space Telescope. *Front. Astron. Space Sci.* **2021**, *8*, 31.
19. Cox, A.N.; Morgan, S.M.; Rogers, F.J.; Iglesias, C.A. An Opacity Mechanism for the Pulsations of OB Stars. *ApJ* **1992**, *393*, 272. [CrossRef]
20. Moskalik, P.; Dziembowski, W.A. New opacities and the origin of the β Cephei pulsation. *A&A* **1992**, *256*, L5–L8.
21. Dziembowski, W.A.; Moskalik, P.; Pamyatnykh, A.A. The opacity mechanism in B-type stars - II. Excitation of high-order g-modes in main-sequence stars. *MNRAS* **1993**, *265*, 588–600. [CrossRef]
22. Salmon, S.; Montalbán, J.; Morel, T.; Miglio, A.; Dupret, M.A.; Noels, A. Testing the effects of opacity and the chemical mixture on the excitation of pulsations in B stars of the Magellanic Clouds. *MNRAS* **2012**, *422*, 3460–3474.
23. Moravveji, E. The impact of enhanced iron opacity on massive star pulsations: updated instability strips. *MNRAS* **2016**, *455*, L67–L71.
24. Walczak, P.; Fontes, C.J.; Colgan, J.; Kilcrease, D.P.; Guzik, J.A. Wider pulsation instability regions for β Cephei and SPB stars calculated using new Los Alamos opacities. *A&A* **2015**, *580*, L9. [CrossRef]
25. Pamyatnykh, A.A.; Handler, G.; Dziembowski, W.A. Asteroseismology of the β Cephei star ν Eridani: Interpretation and applications of the oscillation spectrum. *MNRAS* **2004**, *350*, 1022–1028.
26. Turcotte, S.; Richard, O. Of Variability, or its Absence, in HgMn Stars. *Ap&SS* **2003**, *284*, 225–228.
27. Alecian, G.; Gebran, M.; Auvergne, M.; Richard, O.; Samadi, R.; Weiss, W.W.; Baglin, A. Looking for pulsations in HgMn stars through CoRoT lightcurves. *A&A* **2009**, *506*, 69–78.

28. Morel, T.; Briquet, M.; Auvergne, M.; Alecian, G.; Ghazaryan, S.; Niemczura, E.; Fossati, L.; Lehmann, H.; Hubrig, S.; Ulusoy, C.; et al. A search for pulsations in the HgMn star HD 45975 with CoRoT photometry and ground-based spectroscopy. *A&A* **2014**, *561*, A35.
29. Bourge, P.; Alecian, G.; Thoul, A.; Scuflaire, R.; Theado, S. Radiative forces and pulsation in beta Cephei stars. *Commun. Asteroseismol.* **2006**, *147*, 105–108. [CrossRef]
30. Michaud, G.; Alecian, G.; Richer, J. *Atomic Diffusion in Stars*, *Astronomy and Astrophysics Library*; Springer International Publishing: Cham, Switzerland, 2015. [CrossRef]
31. Théado, S.; Vauclair, S.; Alecian, G.; LeBlanc, F. Influence of Thermohaline Convection on Diffusion-Induced Iron Accumulation in a Stars. *ApJ* **2009**, *704*, 1262–1273.
32. Zemskova, V.; Garaud, P.; Deal, M.; Vauclair, S. Fingering Convection Induced by Atomic Diffusion in Stars: 3D Numerical Computations and Applications to Stellar Models. *ApJ* **2014**, *795*, 118.
33. Deal, M.; Richard, O.; Vauclair, S. Hydrodynamical instabilities induced by atomic diffusion in A stars and their consequences. *A&A* **2016**, *589*, A140.
34. Hui-Bon-Hoa, A.; Vauclair, S. Role of atomic diffusion in the opacity enhancement inside B-type stars. *A&A* **2018**, *610*, L15. [CrossRef]
35. Chapman, S. Thermal diffusion and the stars. *MNRAS* **1917**, *77*, 539. [CrossRef]
36. Chapman, S.; Cowling, T.G. *The Mathematical Theory of non-Uniform Gases*, 3d ed.; Cambridge University Press: Cambridge, UK, 1970.
37. Burgers, J.M. *Flow Equations for Composite Gases*; Academic Press: New York, NY, USA, 1969.
38. Eddington, A.S. *The Internal Constitution of the Stars*; Cambridge University Press: Cambridge, UK,1926.
39. Eddington, A.S. Internal circulation in rotating stars. *MNRAS* **1929**, *90*, 54. [CrossRef]
40. Schatzman, E. Théorie du débit d'énergie des naines blanches. *Annales d'Astrophysique* **1945**, *8*, 143.
41. Michaud, G. Diffusion Processes in Peculiar a Stars. *ApJ* **1970**, *160*, 641. [CrossRef]
42. Turcotte, S.; Richer, J.; Michaud, G.; Iglesias, C.A.; Rogers, F.J. Consistent Solar Evolution Model Including Diffusion and Radiative Acceleration Effects. *ApJ* **1998**, *504*, 539. [CrossRef]
43. Alecian, G.; Michaud, G. About diffusivity, radiative viscosity and particle transport. *A&A* **2005**, *431*, 1–5.
44. Aller, L.H.; Chapman, S. Diffusion in the Sun. *ApJ* **1960**, *132*, 461. [CrossRef]
45. Gonzalez, J.F.; LeBlanc, F.; Artru, M.C.; Michaud, G. Improvements on radiative acceleration calculations in stellar envelopes. *A&A* **1995**, *297*, 223–236.
46. Alecian, G.; Stift, M.J. Radiative accelerations in stars: The effects of magnetic polarisation revisited. *A&A* **2004**, *416*, 703–712. [CrossRef]
47. Seaton, M.J. Radiative accelerations in stellar envelopes. *MNRAS* **1997**, *289*, 700–720. [CrossRef]
48. Alecian, G. Approximate formulae for radiative acceleration in stars. *A&A* **1985**, *145*, 275–277.
49. Alecian, G.; LeBlanc, F. New approximate formulae for radiative accelerations in stars. *MNRAS* **2002**, *332*, 891–900. [CrossRef]
50. LeBlanc, F.; Alecian, G. New method for fast and easy computation of radiative accelerations in stars. *MNRAS* **2004**, *352*, 1329–1334. [CrossRef]
51. Alecian, G.; LeBlanc, F. An improved parametric method for evaluating radiative accelerations in stellar interiors. *MNRAS* **2020**, *498*, 3420–3428.
52. Deal, M.; Alecian, G.; Lebreton, Y.; Goupil, M.J.; Marques, J.P.; LeBlanc, F.; Morel, P.; Pichon, B. Impacts of radiative accelerations on solar-like oscillating main-sequence stars. *A&A* **2018**, *618*, A10.
53. Schatzman, E. Gravitational Separation of the Elements and Turbulent Transport. *A&A* **1969**, *3*, 331.
54. Richer, J.; Michaud, G.; Turcotte, S. The Evolution of AMFM Stars, Abundance Anomalies, and Turbulent Transport. *ApJ* **2000**, *529*, 338–356. [CrossRef]
55. Michaud, G.; Richer, J.; Vick, M. Sirius A: Turbulence or mass loss? *A&A* **2011**, *534*, A18.
56. Alecian, G.; Stift, M.J. Time-dependent atomic diffusion in the atmospheres of CP stars. A big step forward: Introducing numerical models including a stellar mass-loss. *MNRAS* **2019**, *482*, 4519–4527. [CrossRef]
57. Morel, P.; Lebreton, Y. CESAM: A free code for stellar evolution calculations. *Astrophys. Space Sci.* **2008**, *316*, 61–73.
58. Marques, J.P.; Goupil, M.J.; Lebreton, Y.; Talon, S.; Palacios, A.; Belkacem, K.; Ouazzani, R.M.; Mosser, B.; Moya, A.; Morel, P.; et al. Seismic diagnostics for transport of angular momentum in stars. I. Rotational splittings from the pre-main sequence to the red-giant branch. *A&A* **2013**, *549*, A74.
59. Ryabchikova, T. Direct evidence for stratification in A/B stellar atmospheres. In Proceedings of the European Astronomical Society Publications Series, EDP Science, Chateau de Mons, France, 6–10 June 2005; Alecian, G., Richard, O., Vauclair, S., Eds.; 2005; Volume 17, pp. 253–262. [CrossRef]
60. Alecian, G.; Stift, M.J. 3D distribution models of Ca, Cr, and Fe in a magnetic CP star atmosphere with anisotropic wind. *MNRAS* **2021**, *504*, 1370–1378. [CrossRef]
61. Michaud, G.; Richer, J.; Richard, O. Horizontal Branch Evolution and Atomic Diffusion. *ApJ* **2007**, *670*, 1178–1187. [CrossRef]
62. Proffitt, C.R.; Vandenberg, D.A. Implications of Helium Diffusion for Globular Cluster Isochrones and Luminosity Functions. *ApJS* **1991**, *77*, 473. [CrossRef]

63. Vandenberg, D.A.; Bolte, M.; Stetson, P.B. The Age of the Galactic Globular Cluster System. *Annu. Rev. Astron. Astrophys.* **1996**, *34*, 461–510. [CrossRef]
64. Michaud, G.; Richer, J. Horizontal branch stars as AmFm/HgMn stars. *Contrib. Astron. Obs. Skaln. Pleso* **2008**, *38*, 103–112.
65. Behr, B.B. Rotation Velocities of Red and Blue Field Horizontal-Branch Stars. *ApJS* **2003**, *149*, 101–121.
66. Khalack, V.R.; Leblanc, F.; Behr, B.B.; Wade, G.A.; Bohlender, D. Search for vertical stratification of metals in atmospheres of blue horizontal-branch stars. *A&A* **2008**, *477*, 641–647. [CrossRef]
67. Hui-Bon-Hoa, A.; LeBlanc, F.; Hauschildt, P.H. Diffusion in the Atmospheres of Blue Horizontal-Branch Stars. *ApJ* **2000**, *535*, L43–L45. [CrossRef] [PubMed]
68. LeBlanc, F.; Monin, D.; Hui-Bon-Hoa, A.; Hauschildt, P.H. Stellar model atmospheres with abundance stratification. *A&A* **2009**, *495*, 937–944. [CrossRef]
69. Leblanc, F.; Hui-Bon-Hoa, A.; Khalack, V.R. Stratification of the elements in the atmospheres of blue horizontal-branch stars. *MNRAS* **2010**, *409*, 1606–1610.
70. Schatzman, E.L. *White Dwarfs*; North-Holland Publishing Company: Amsterdam, The Netherlands, 1958.
71. Fontaine, G.; Michaud, G. Diffusion time scales in white dwarfs. *ApJ* **1979**, *231*, 826–840. [CrossRef]
72. Turcotte, S.; Richer, J.; Michaud, G. Consistent Evolution of F Stars: Diffusion, Radiative Accelerations, and Abundance Anomalies. *ApJ* **1998**, *504*, 559–572. [CrossRef]
73. Richard, O.; Michaud, G.; Richer, J. Iron Convection Zones in B, A, and F Stars. *ApJ* **2001**, *558*, 377–391. [CrossRef]
74. Deal, M.; Goupil, M.J.; Marques, J.P.; Reese, D.R.; Lebreton, Y. Chemical mixing in low mass stars. I. Rotation against atomic diffusion including radiative acceleration. *A&A* **2020**, *633*, A23.
75. Lucy, L.B.; Solomon, P.M. Mass Loss by Hot Stars. *ApJ* **1970**, *159*, 879. [CrossRef]
76. Castor, J.I.; Abbott, D.C.; Klein, R.I. Radiation-driven winds in Of stars. *ApJ* **1975**, *195*, 157–174. [CrossRef]
77. Abbott, D.C. The theory of radiatively driven stellar winds. II. The line acceleration. *ApJ* **1982**, *259*, 282–301. [CrossRef]
78. Babel, J. Multi-component radiatively driven winds from A and B stars. I. The metallic wind of a main sequence A star. *A&A* **1995**, *301*, 823.
79. Krtička, J.; Kubát, J. Multicomponent radiatively driven stellar winds. I. Nonisothermal three-component wind of hot B stars. *A&A* **2001**, *369*, 222–238. [CrossRef]
80. Krtička, J.; Kubát, J.; Groote, D. Multicomponent radiatively driven stellar winds. *Astron. Astrophys.* **2006**, *460*, 145–153. [CrossRef]
81. Fišák, J.; Kubát, J.; Kubátová, B.; Kromer, M.; Krtička, J. Progress towards a 3D Monte Carlo radiative transfer code for outflow wind modelling. *arXiv* **2022**, arXiv:2212.11016. [CrossRef]
82. Nsamba, B.; Campante, T.L.; Monteiro, M.J.P.F.G.; Cunha, M.S.; Rendle, B.M.; Reese, D.R.; Verma, K. Asteroseismic modelling of solar-type stars: Internal systematics from input physics and surface correction methods. *MNRAS* **2018**, *477*, 5052–5063.
83. Mombarg, J.S.G.; Dotter, A.; Van Reeth, T.; Tkachenko, A.; Gebruers, S.; Aerts, C. Asteroseismic Modeling of Gravity Modes in Slowly Rotating A/F Stars with Radiative Levitation. *ApJ* **2020**, *895*, 51.